

TRACKING MULTIPLE CLOSELY SPACED TARGETS USING AN ADAPTIVE FOVEAL SENSOR

Fengjun Xi and Darryl Morrell

Department of Electrical Engineering
Arizona State University
Fengjun.Xi@asu.edu, morrell@asu.edu

ABSTRACT

We address the problem of configuring a foveal sensor to track multiple, closely spaced moving targets. The foveal sensor has a high acuity region, whose center and extent can be configured, surrounded by a low acuity region. We study three heuristic approaches to extend a near-optimal greedy configuration rule for a single target to multiple targets: simultaneously observe all targets (SO), center the foveal region on each target in turn (TO), and center the foveal region on the target with the worst position estimate (WO). The target tracker is implemented using a particle filter with joint probabilistic data association (JPDA). Additionally, we implement two different independent-partition proposal distributions using JPDA and global nearest neighbor (GNN). Monte Carlo simulations show that the WO rule outperforms the other rules and that the IP-JPDA proposal gives better tracking performance.

I. INTRODUCTION

Tracking multiple, closely-spaced targets using an attentive sensor in heavy clutter is a challenging problem. Previous work [1, 2] developed attentive sensor control strategies to track single target. In this paper, we investigate strategies to track multiple targets moving in one dimension with a foveal sensor. The foveal sensor has a high acuity region, whose center and extent can be configured, surrounded by a low acuity region; target positions within the high acuity foveal region are observed more accurately. The control strategies are obtained by extending a near-optimal, greedy algorithm from single target to multiple targets using three approaches: simultaneously observe all targets (SO), center the foveal region on each target in turn (TO), and center the foveal region on the target with the worst position estimate (WO). The target tracker is implemented using a joint multi-target probability density (JMPD) particle filter with joint probabilistic data association (JPDA). Our simulation results show the best performance is obtained by the WO rule.

This work supported by AFOSR under grant F49620-03-1-0117.

A second contribution of this paper is a novel independent partition (IP) proposal scheme for the particle filter. Previous work [3, 4] developed the independent partition method to reduce the number of particles (and hence the computational burden) necessary to implement the particle filter. That work used sensor arrays and unified target tracking (i.e. tracking with sensor models that do not require data association). We have adapted the IP proposal method to include data association using two different methods: GNN and JPDA. IP-JPDA provides better performance in the presence of clutter.

The rest of this paper is organized as follows: Section II describes the target dynamics and observation models. Section III briefly outlines the tracker algorithm. We present three foveal sensor configuration algorithms in Section IV, and introduce the IP-JPDA and IP-GNN proposal schemes in Section V. Section VI compares the three configuration algorithms as well as IP-GNN and IP-JPDA through Monte Carlo simulations. Conclusions are given in Section VII.

II. TARGET DYNAMICS AND SENSOR MODELS

We consider T_{max} targets moving in one dimension. Let \mathbf{x}_k^t denote the state vector of target t at discrete time k :

$$\mathbf{x}_k^t = [X_k^t \quad \dot{X}_k^t]^\top.$$

where X_k^t is position and \dot{X}_k^t is velocity. The state vector for a given target is also called a partition. We use a constant velocity target motion model:

$$\mathbf{x}_k^t = \begin{bmatrix} 1 & \Delta t \\ 0 & 1 \end{bmatrix} \mathbf{x}_{k-1}^t + \mathbf{n}_{k-1}^t,$$

where Δt is the time difference between measurements, and \mathbf{n}_{k-1}^t is a zero-mean Gaussian process with covariance Q . The multitarget state vector for T_{max} targets is composed of the individual partitions:

$$\mathbf{x}_k = [\mathbf{x}_k^1 \top, \mathbf{x}_k^2 \top, \dots, \mathbf{x}_k^{T_{max}} \top]^\top.$$

The foveal sensor provides observations of the target position corrupted by noise. The sensor has two adjustable parameters: d_k sets the location of the foveal region, while c_k sets the gain at the center of the foveal region. The observation for target t is obtained from its position as

$$z_k = \arctan(c_k[X_k^t - d_k]) + v_k^t,$$

where v_k^t is white Gaussian noise with variance R .

Once configured, the foveal sensor provides measurements of target positions; it detects each target with a known probability P_D . The measurement vector at time k is $\mathbf{z}_k = [z_k^1, z_k^2, \dots, z_k^{M_k}]^\top$. Its elements consist of observed target positions and clutter. We model clutter as uniformly distributed over the surveillance region volume \mathbf{V} ; the number of false alarms is Poisson distributed with parameter $\lambda\mathbf{V}$, where λ is the spatial false alarm density and is known to the tracker.

III. TRACKER ALGORITHM

The nonlinearity of the foveal sensor observation model necessitates the use of a particle filter in this application. We use Monte Carlo joint probabilistic data association [5] and an independent partition proposal distribution (described in Section V) to estimate the target state and provide information necessary to configure the foveal sensor. The posterior distribution of \mathbf{x}_k given \mathbf{z}_1 through \mathbf{z}_k is approximated by T_{max} sets of N_{part} particles $\{\mathbf{x}_k^i\}_{i=1}^{N_{part}}$ and associated weights $\{\omega_k^i\}_{i=1}^{N_{part}}$. Table 1 outlines our tracking algorithm.

IV. SENSOR CONFIGURATION

We improved the performance of the single-target configuration rule in [1] by examining the characteristics of the near-optimal solution obtained using SPSA [7] for $R \in [0, 0.4]$. The foveal center d is positioned at the predicted target position. The foveal gain c is set to

$$c = \begin{cases} \frac{\pi}{\sqrt{P^+(-1.8 \log_{10} R)}}, & 0.4 \geq R \geq 0.0146 \\ \frac{\pi}{3.30\sqrt{P^+}}, & 0 \leq R < 0.0146 \end{cases} \quad (1)$$

where P^+ is the predicted position error variance.

From this single target rule, we have developed three foveal sensor configuration rules for multi-target tracking. SO is designed to observe all targets at the same time. In order to let all targets fall within the high acuity foveal region, d is set to the point midway between the two most widely separated targets (say, i and j). Denoting the distance between targets i and j as D_{ij} , we set the gain as:

$$c = \begin{cases} \frac{\pi}{(D_{ij} + 0.9(\sqrt{P_i^+} + \sqrt{P_j^+}))(-\log_{10} R)}, & 0.4 \geq R \geq 0.0146 \\ \frac{\pi}{(D_{ij} + 1.65(\sqrt{P_i^+} + \sqrt{P_j^+}))}, & 0 \leq R < 0.0146 \end{cases}$$

Table 1. Multiple Target Tracking Algorithm

1. Generate $\{\mathbf{x}_0^i\}_{i=1}^{N_{part}}$; set $\{\omega_0^i\}_{i=1}^{N_{part}} = \frac{1}{N_{part}}$.
2. Compute $\hat{\mathbf{x}}_0 = \sum_{i=1}^{N_{part}} \omega_0^i \mathbf{x}_0^i$ and $\hat{P}_0 = \sum_{i=1}^{N_{part}} \omega_0^i (\mathbf{x}_0^i - \hat{\mathbf{x}}_0)(\mathbf{x}_0^i - \hat{\mathbf{x}}_0)^T$.
3. Set $k = 1$.
4. Compute the predicted state estimate $\hat{\mathbf{x}}_k^+ = F\hat{\mathbf{x}}_{k-1}$ and predicted error covariance $P_k^+ = F\hat{P}_{k-1}F^T + Q$.
5. Configure d_k and c_k as in Section IV.
6. Obtain \mathbf{z}_k using the configured sensor.
7. For each target t , propose a set of partitions $\{\mathbf{x}_k^{t,i}\}_{i=1}^{N_{part}}$ and associated bias terms $\{b_k^{t,i}\}_{i=1}^{N_{part}}$ via the IP-GNN or IP-JPDA algorithm of Section V; concatenate all partitions to form particles $\mathbf{x}_k^i = [\mathbf{x}_k^{1,i^\top}, \mathbf{x}_k^{2,i^\top}, \dots, \mathbf{x}_k^{T_{max},i^\top}]^\top$.
8. For $i = 1, \dots, N_{part}$,

$$\omega_k^i = \omega_{k-1}^i \frac{\sum_{l=1}^{N_H} p(\mathbf{z}_k, \pi_k^l | \mathbf{x}_k^i)}{\prod_{t=1}^{T_{max}} b_k^{t,i}}$$

where $\{\pi_k^l\}_{l=1}^{N_H}$ is the set of feasible associations of observations to targets, N_H is the total number of feasible hypotheses, and $p(\mathbf{z}_k, \pi_k^l | \mathbf{x}_k^i)$ is given in [5].

9. For $i = 1, \dots, N_{part}$, normalize weights

$$\omega_k^i = \frac{\omega_k^i}{\sum_{i=1}^{N_{part}} \omega_k^i}$$

10. Permute particles by the K-means algorithm[4].
11. Compute the state estimate $\hat{\mathbf{x}}_k = \sum_{i=1}^{N_{part}} \omega_k^i \mathbf{x}_k^i$, error covariance $\hat{P}_k = \sum_{i=1}^{N_{part}} \omega_k^i (\mathbf{x}_k^i - \hat{\mathbf{x}}_k)(\mathbf{x}_k^i - \hat{\mathbf{x}}_k)^T$.
12. Calculate $\hat{N}_{eff} = \frac{1}{\sum_{i=1}^{N_{part}} (\omega_k^i)^2}$ and perform resampling if $\hat{N}_{eff} < N_T$.
13. Set $k \leftarrow k + 1$ and go to step 4.

where P_i^+ and P_j^+ are the predicted position error variances of targets i and j . In TO, the foveal region is centered on each target in turn, while the gain is computed using (1) with P^+ of the centered target. In WO, the foveal region is centered on the target that has the largest predicted position error variance, and the gain is also computed using (1) with P^+ of the centered target.

V. INDEPENDENT PARTITION PROPOSALS

The independent partition approach proposes a collection of particles for each partition $\{\mathbf{x}_k^{t,i^*}\}_{i=1}^{N_{part}}$; weights $\{\omega_k^{t,i}\}_{i=1}^{N_{part}}$, which depend on the observation \mathbf{z}_k , are com-

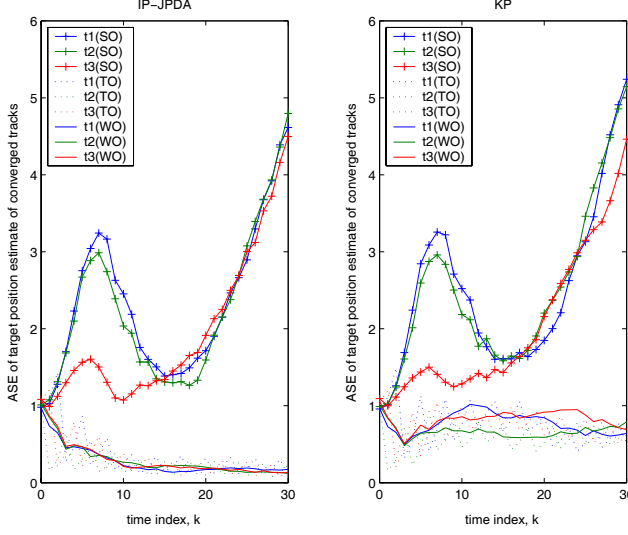


Fig. 1. Average squared position error (ASE) for three targets (t1, t2, and t3) for the SO, TO and WO heuristics with no clutter.

puted for each partition. Computation of the weight requires that the elements of \mathbf{z}_k be associated with each partition. The proposed particles for each partition are resampled according to these weights to obtain a collection $\{\mathbf{x}_k^{t,i}\}_{i=1}^{N_{part}}$. These partitions are arranged into particles: $\mathbf{x}_k^i = [\mathbf{x}_k^{1,i\top}, \mathbf{x}_k^{2,i\top}, \dots, \mathbf{x}_k^{T_{max},i\top}]^\top$. We investigate two association approaches to implement IP proposal distributions: global nearest neighbor (IP-GNN) and joint probabilistic data association (IP-JPDA).

The GNN method makes one-to-one assignments between the elements of \mathbf{z}_k and the partitions $\mathbf{x}_k^{t,i}$ of particle \mathbf{x}_k^i to minimize the total distance between measurements and predicted measurements [6]. The set of assignments is then used to compute the weight assigned to each partition.

The JPDA method computes weights for a given partition $\mathbf{x}_k^{t,i}$ by applying JPDA as if it were the only target present (treating observations from other targets as false alarms).. This requires enumerating all association hypotheses between $\mathbf{x}_k^{t,i}$ and the elements of \mathbf{z}_k ; we denote the set of possible hypothesis as $\{\pi_k^{t,l}\}_{l=1}^{N_{Hpart}}$. Here, N_{Hpart} is the total number of association hypotheses for the partition $\mathbf{x}_k^{t,i}$. Table 2 shows the details of the IP-JPDA proposal scheme.

VI. SIMULATION RESULTS

We evaluated performance by examining the percentage of Monte Carlo runs in which the tracker converges (i.e. position errors for all targets remain below a given threshold during the last ten time steps of each run) and, for converged runs, the average squared error (ASE) in the estimated posi-

Table 2. IP-JPDA Subroutine for Target t

1. For each particle $i = 1, \dots, N_{part}$,
 - (a) Sample $\mathbf{x}_k^{t,i*} \sim p(\mathbf{x}_k | \mathbf{x}_{k-1}^{t,i})$
 - (b) For each $\pi_k^{t,l}$, compute $p(\mathbf{z}_k, \pi_k^{t,l} | \mathbf{x}_k^{t,i*})$
 - (c) Compute $w_k^{t,i} = \sum_{l=1}^{N_{Hpart}} p(\mathbf{z}_k, \pi_k^{t,l} | \mathbf{x}_k^{t,i*})$
2. Normalize $\{w_k^{t,i}\}_{i=1}^{N_{part}}$ to sum to 1
3. For each particle $i = 1, \dots, N_{part}$, sample an index j according to the distribution $\{w_k^{t,i}\}_{i=1}^{N_{part}}$; set $\mathbf{x}_k^{t,i} = \mathbf{x}_k^{t,j*}$ and $b_k^{t,i} = w_k^{t,j}$.

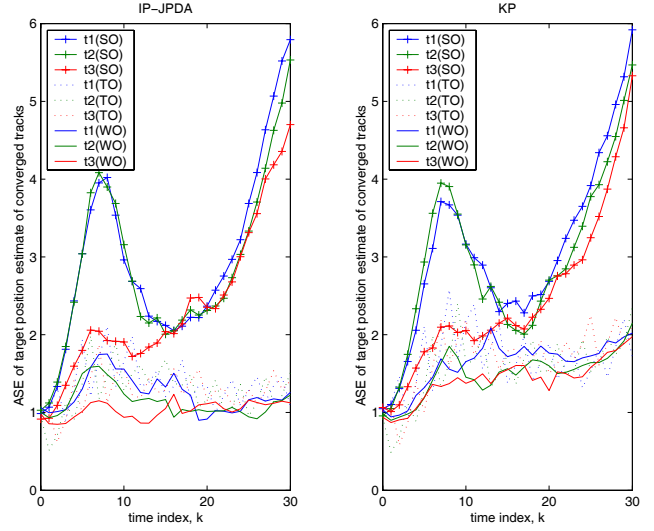


Fig. 2. ASE for the SO, TO and WO heuristics in clutter.

tion of each target. All evaluations used 1000 Monte Carlo simulation runs with $q = 0.01$, $R = 0.05$, $\Delta t = 1$, and $N_{part} = 400$. The initial particles were sampled from a Gaussian distribution whose mean is the true targets' state \mathbf{x}_0 and whose covariance is $P_0 = \text{diag}(1, 0.1)$.

We compared the performance of the SO, TO, and WO approaches for both IP-JPDA and kinematic prior (KP) proposals for no clutter ($P_D = 1$, $\lambda\mathbf{V} = 0$) and clutter ($P_D = 0.9$, $\lambda\mathbf{V} = 0.5$). Table 3 and Fig. 1 show percent convergence and ASE as a function of time for the SO, TO and WO heuristics tracking three targets in no clutter. Table 4 and Fig. 2 show the corresponding performance with clutter. The performance of IP-JPDA is always better than that of KP, and WO and TO with IP-JPDA proposal perform better than SO. Also, WO appears to be generally slightly better than TO in the presence of clutter.

We also compared IP-JPDA and IP-GNN. Table 5 and Fig. 3 show that IP-JPDA has the same performance tracking 2 targets as IP-GNN when $P_D = 1$ and $P_{FA} = 0$; while IP-JPDA has better performance than IP-GNN when

Table 3. Percentage of runs that converged with no clutter

Proposal method	SO	TO	WO
IP-JPDA	90.5%	99.5%	99.7%
KP	88.5%	97.1%	96.4%

Table 4. Percentage of runs that converged in clutter

Proposal method	SO	TO	WO
IP-JPDA	81.1%	90.7%	92.5%
KP	80.6%	75.8%	83.1%

$P_D = 0.9$ and $\lambda V = 0.5$. This is because IP-JPDA can counteract the negative influence of false measurement-to-target assignments. To further test the robustness of IP-JPDA, we applied it to two different scenarios in clutter in which three moving targets have different initial positions and velocities. Fig. 4 shows the true and estimated trajectories; the IP-JPDA proposal scheme works for both cases.

VII. CONCLUSIONS

In this paper, we introduce an attentive tracker for multiple closely spaced targets using an adaptive foveal sensor. Three foveal sensor configuration rules are studied and compared by Monte Carlo simulations. The WO rule generally outperforms the TO and SO rules for either IP-JPDA or KP proposals. In addition, both IP-JPDA and IP-GNN proposal approaches are presented and investigated. Monte Carlo simulations show better performance is obtained by IP-JPDA than by IP-GNN in the presence of clutter.

VIII. REFERENCES

- [1] Y. Xue and D. Morrell, "Adaptive Foveal Sensor for Target Tracking," *36th Asilomar Conf. on Sig., Sys., and Comp.*, pp. 848-852, Nov. 2002.
- [2] H. Shah and D. Morrell, "An Adaptive Zoom Algorithm For Tracking Targets Using Pan-Tilt-Zoom Cameras," *ICASSP'04*, May 2004.
- [3] M. Orton and W. Fitzgerald, "A Bayesian Approach to Tracking Multiple Targets Using Sensor Arrays and Particle Filters," *IEEE Tran. Sig. Proc.*, vol. 50, no. 2, pp. 216-223, Feb. 2002.
- [4] C. Kreucher, K. Kastella, A. O. Hero, "Tracking Multiple Targets Using a Particle Filter Representation of the

Table 5. Percentage of runs that converged using IP-JPDA and IP-GNN

Proposal method	no clutter	clutter
IP-JPDA	100%	98.9%
IP-GNN	100%	84.1%

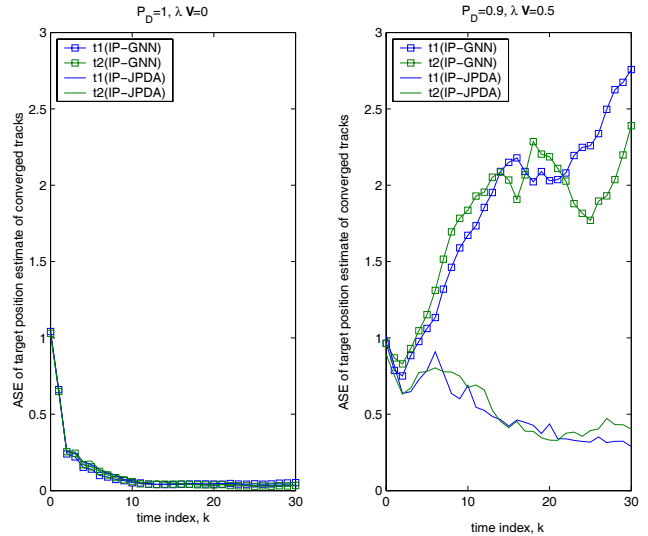


Fig. 3. Comparison between IP-JPDA and IP-GNN proposal schemes for clutter and no clutter.

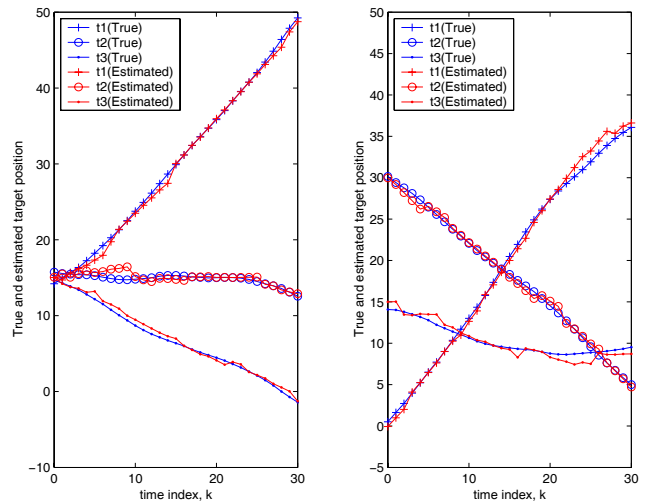


Fig. 4. True and estimated trajectories using IP-JPDA

- [5] Joint Multitarget Probability Density," *SPIE Intl. Symposium on Opt. Sci. and Tech.*, San Diego, CA, Aug. 2003
- [6] R. Karlsson and F. Gustafsson, "Monte Carlo data association for multiple target tracking," *Proc. of IEE Target Tracking: Algorithms and Applications*, vol. 1, pp. 13/1-13/5, Oct. 2001.
- [7] S. Blackman and R. Popoli, *Design and Analysis of Modern Tracking Systems*, Artech House, 1999.
- [8] J. C. Spall, "An Overview of the Simultaneous Perturbation Method for Efficient Optimization," *Johns Hopkins APL Technical Digest*, vol. 19, No. 4, 1998.